Vehicle Attitude Control with Saturating Actuators: Workload Balancing and Reference Adaptation

A. Borri, D. Bianchi, M. D. Di Benedetto and S. Di Gennaro

***Abstract*— This paper addresses the problem of vehicle attitude control in the presence of saturating actuators. A novel approach of actuation balancing is proven to be the best way to keep the vehicle off saturation or, at least, to postpone the saturation occurrences as late as possible. In hard conditions, this may be not sufficient to guarantee tracking; hence the joint design of a load-balancing control law and an adapted reference generator is addressed, in order to cope with the lack in the control action and prevent unstable behaviors. On top of the formal results, the method is validated by means of simulations.**

I. Introduction

Active attitude control systems and their integration is one of the main research areas in vehicle control. Different active technologies (active braking, active steering, active differential) have been developed and applied in different control schemes (see e.g. [1], [2], [3], [4], [5], [6]). Most of the aforementioned work did not consider explicitly the issue of actuator saturation, which limits the maximum obtainable performance of mechanical actuators operating under physical constraints. In an integrated control structure more degrees of freedom are available for control, thus potentially limiting the saturation occurrences.

The problem of input saturation has received increasing attention in the control research community. Comprehensive overviews of modern anti-windup approaches are given in [7], [8]. In vehicle control, the basic approaches to deal with input saturations aim either at preventing saturations or at managing the occurrence of saturations. A discussion of robust control techniques (including Internal Model Control, H_∞ optimization, and anti-windup schemes) applied to vehicular systems can be found in [9]. In [10]–[11], the authors of the present work proposed some approaches to the management of the actuator saturations, based on priority schemes, input limiting functions and/or on a modification of the reference signal. Although the solutions there presented ensure good tracking performances, the problem of the closed-loop stability of the resulting hybrid system in the presence of discontinuity of the control actions remained, in general, an open problem.

The research leading to these results has received funding from the European Union Seventh Framework Programme [FP7/2007–2013] under grant agreement No. 257462 HYCON2 Network of excellence.

A. Borri is with the Istituto di Analisi dei Sistemi ed Informatica "A. Ruberti", Consiglio Nazionale delle Ricerche (IASI-CNR), Viale Manzoni 30, 00185 Rome, Italy. E-mail: alessandro.borri@iasi.cnr.it.

D. Bianchi, M. D. Di Benedetto and S. Di Gennaro are with the Department of Information Engineering, Computer Science and Mathematics; they are also with the Center of Excellence DEWS, University of L'Aquila, Via Vetoio, Loc. Coppito, 67100 L'Aquila, Italy. E-mail: {domenico.bianchi, mariadomenica.dibenedetto, stefano.digennaro}@univaq.it.

In this paper, an integrated control scheme of Active Front Steer (AFS) and Rear Torque Vectoring (RTV) is considered. The contribution is two-fold:

1) a control law, achieving balancing of the workload on the actuators, is designed and exponential tracking is shown in nominal (non-saturated) conditions. Load balancing is a principle that is common to different fields in engineering in order to optimally distribute the workload across multiple resources, balance the utilization, increase reliability, and avoid overload. We pose the balancing problem and solve it as an optimization problem, whose goal is the guarantee that both the actuators keep as far away as possible from saturation conditions;
2) we use the idea in [11] of modifying the reference generator, with a different approach. We show how to modify the reference in order to compensate the lack of control action of saturated actuators, while fulfilling the physical constraints. We obtain a continuous control action and achieve the tracking goal.

The paper is organized as follows. Section II illustrates the vehicle model. In Section III, a control law is designed to achieve exponential tracking of a reference vehicle model, in the presence of unbounded inputs, also achieving load balancing between the two actuations. Section IV addresses the adaptation of the reference generator when saturation conditions occur. Section V illustrates some simulation results. Section VI includes final remarks.

II. Vehicle Model

In the modeling phase, we consider the classical single–track vehicle model with two degrees of freedom: the lateral velocity v_y (m/s) and the yaw rate ω_z (rad/s). Although simple, this model well captures the major features of interest of a vehicle for the analysis and the control design and its simplifying assumptions are verified in a large number of situations (see e.g. [6] for further considerations). The dynamic equations are

$$\begin{aligned} m(\dot{v}_y + v_x\omega_z) &= \mu(F_{yf} + F_{yr}), \\ J_z\dot{\omega}_z &= \mu(F_{yf}l_f - F_{yr}l_r) + M_z, \end{aligned} \tag{1}$$

where m is the vehicle mass (kg), J_z is the vehicle inertia momentum (kg m^2), v_x is the vehicle longitudinal velocity (m/s), l_f, l_r are the distances from the center of gravity to the front and rear axle (m), F_{yf}, F_{yr} are the front/rear tire lateral forces (N), M_z is the RTV yaw moment (N m), μ is the tire–road friction coefficient (dimensionless).

Preprint submitted to 52nd IEEE Conference on Decision and Control .
Received March 11, 2013.

The actuators considered in this work are:

- Active Front Steer (AFS), which imposes an incremental steer angle on top of the driver's input. The control is then actuated through the front axle tire characteristic.
- Rear Torque Vectoring (RTV), which distributes the torque in the rear axle, usually to improve vehicle traction, handling and stability. The control is then actuated through the rear axle tire characteristics.

The front/rear lateral forces

$$F_{yf} = F_{yf}(\alpha_f), \quad F_{yr} = F_{yr}(\alpha_r)$$

depend on the front/rear tire slip angles (rad)

$$\alpha_f = \delta - \frac{v_y + l_f\omega_z}{v_x}, \quad \alpha_r = -\frac{v_y - l_r\omega_z}{v_x},$$

with $\delta = \delta_d + \delta_c$ the road wheel angle (rad), sum of the driver angle δ_d (rad) and the AFS angle δ_c (rad). The drive angle δ_d is assumed at least continuous with respect to time.

The tire lateral behavior can be represented by some functions describing the dependence on the slip angle (see, for instance [12]). The tires determine a force in the direction of the slip angles, which contrasts the drift of the wheel, but this force decreases after a certain value of the slip angle, as in the following function:

$$F_{yf}(\alpha_f) = F_{yf,\mathrm{sat}}F_{yf,n}(\alpha_f), \quad F_{yr}(\alpha_r) = F_{yr,\mathrm{sat}}F_{yr,n}(\alpha_r),$$

where $F_{yf,n}$ and $F_{yr,n}$ are normalized odd functions (e.g. the Pacejka's magic formulas) with global maxima $F_{yf,\mathrm{sat}}, F_{yr,\mathrm{sat}} > 0$ at the saturation points $\alpha_{f,\mathrm{sat}}$ and $\alpha_{r,\mathrm{sat}}$.

The actuations in the vehicle dynamics (1) are the AFS angle δ_c and the RTV yaw moment M_z. The former can be computed inverting the function $F_{y,f}$. This can be done up to the tire saturation point $\alpha_{f,\mathrm{sat}}$ and saturating the inverse function elsewhere, i.e.

$$\delta_c = \begin{cases} -\delta_d + \dfrac{v_y + l_f\omega_z}{v_x} + F_{yf}^{-1}(F_0), & |F_0| \le F_{yf,\mathrm{sat}} \\ -\delta_d + \dfrac{v_y + l_f\omega_z}{v_x} + \alpha_{f,\mathrm{sat}}, & \text{otherwise} \end{cases}$$

for a given value F_0. In order to deal with simpler quantities, one can use simple algebraic manipulations and define the following control input:

$$\Delta_c = F_{yf}(\alpha_f) - F_{yf}(\alpha_{f0}), \tag{2}$$

with

$$\alpha_{f0} = \delta_d - \frac{v_y + l_f\omega_z}{v_x}.$$

Hence, the equations in (1) can be rewritten in the form

$$\begin{aligned} \dot v_y &= -v_x\omega_z + \frac{\mu}{m}\Big(F_{yf}(\alpha_{f0}) + F_{yr}(\alpha_r)\Big) + \frac{\mu}{m}\Delta_c, \\ \dot\omega_z &= \frac{\mu}{J_z}\Big(F_{yf}(\alpha_{f0})l_f - F_{yr}(\alpha_r)l_r\Big) + \frac{\mu l_f}{J_z}\Delta_c + \frac{1}{J_z}M_z. \end{aligned} \tag{3}$$

The *control problem* is the asymptotic tracking of some bounded reference states $v_{y,\mathrm{ref}}$ and $\omega_{z,\mathrm{ref}}$, which are assumed to have bounded derivatives. The reference generator is described later in the paper. In order words, we address the control design problem for the actuators AFS and RTV such that the error dynamics

$$e_{v_y} = v_y - v_{y,\mathrm{ref}}, \qquad e_{\omega_z} = \omega_z - \omega_{z,\mathrm{ref}} \tag{4}$$

tend to zero asymptotically and uniformly.

In the following sections, we will address the solution of the control problem. We first design the control in nominal condition, without considering any bounds on the actuations.

III. Tracking with balanced actuators in nominal conditions

The reference dynamics to be tracked are

$$\begin{aligned} \dot v_{y,\mathrm{ref}} &= -v_x\omega_{z,\mathrm{ref}} + \frac{\mu}{m}\Big(F_{yf,\mathrm{ref}}(\alpha_{f0,\mathrm{ref}}) + F_{yr,\mathrm{ref}}(\alpha_{r,\mathrm{ref}})\Big), \\ \dot\omega_{z,\mathrm{ref}} &= \frac{\mu}{J_z}\Big(F_{yf,\mathrm{ref}}(\alpha_{f0,\mathrm{ref}})l_f - F_{yr,\mathrm{ref}}(\alpha_{r,\mathrm{ref}})l_r\Big), \\ \alpha_{f0,\mathrm{ref}} &= \delta_d - \frac{v_{y,\mathrm{ref}} + l_f\omega_{z,\mathrm{ref}}}{v_x}, \\ \alpha_{r,\mathrm{ref}} &= -\frac{v_{y,\mathrm{ref}} - l_r\omega_{z,\mathrm{ref}}}{v_x}. \end{aligned} \tag{5}$$

The reference trajectory generator above is assumed to have a globally asymptotically stable equilibrium at the origin. One can show (see e.g. [13]) that a sufficient condition to obtain such a property is that the functions $F_{yf,\mathrm{ref}}$ and $F_{yf,\mathrm{ref}}$ have a strictly positive derivative with respect to $\alpha_{f,\mathrm{ref}}$ and $\alpha_{r,\mathrm{ref}}$.

A. Classical Nonlinear Global Stabilization

From (3), (4), (5), the tracking error dynamics are

$$\begin{aligned} \dot e_{v_y} &= -v_x e_{\omega_z} + \frac{\mu}{m}(E_f + E_r) + \frac{\mu}{m}\Delta_c, \\ \dot e_{\omega_z} &= \frac{\mu}{J_z}(E_f l_f - E_r l_r) + \frac{\mu l_f}{J_z}\Delta_c + \frac{1}{J_z}M_z, \end{aligned} \tag{6}$$

with

$$\begin{aligned} E_f(\alpha_{f0}, \alpha_{f0,\mathrm{ref}}) &= F_{yf}(\alpha_{f0}) - F_{yf,\mathrm{ref}}(\alpha_{f0,\mathrm{ref}}), \\ E_r(\alpha_r, \alpha_{r,\mathrm{ref}}) &= F_{yr}(\alpha_r) - F_{yr,\mathrm{ref}}(\alpha_{r,\mathrm{ref}}). \end{aligned} \tag{7}$$

The control inputs

$$\begin{aligned} \Delta_c^\circ &= -\frac{m}{\mu}k_1 e_{v_y} + \frac{mv_x}{\mu}e_{\omega_z} - (E_f + E_r), \\ M_z^\circ &= -J_z k_2 e_{\omega_z} - \mu(E_f l_f - E_r l_r) - \mu l_f \Delta_c^\circ \\ &= m l_f k_1 e_{v_y} - J_z k_2 e_{\omega_z} - m v_x l_f e_{\omega_z} + \mu(l_f + l_r)E_r, \end{aligned} \tag{8}$$

with $k_1, k_2 > 0$, ensure the closed–loop global exponential stability (GES) of the error dynamics

$$\begin{pmatrix} \dot e_{v_y} \\ \dot e_{\omega_z} \end{pmatrix} = -\begin{pmatrix} k_1 & 0 \\ 0 & k_2 \end{pmatrix}\begin{pmatrix} e_{v_y} \\ e_{\omega_z} \end{pmatrix}.$$

Preprint submitted to 52nd IEEE Conference on Decision and Control .
Received March 11, 2013.

B. Balanced Nonlinear Global Stabilization

By applying the nominal inputs in (8), it may occur that one actuation is overloaded (and possibly reaches the saturation limit), while the other one is underused. We now design a control action which is able to perfectly balance the workload between AFS and RTV, in order to keep the actuations as far away as possible from saturation. This can be simply done by imposing (6) equal to

$$\begin{pmatrix} \dot{e}_{v_y} \\ \dot{e}_{\omega_z} \end{pmatrix} = - \begin{pmatrix} k_1 & k(t) \\ -k(t) & k_2 \end{pmatrix} \begin{pmatrix} e_{v_y} \\ e_{\omega_z} \end{pmatrix} \tag{9}$$

with $k(t) \in \mathbb{R}$, obtaining

$$\begin{aligned} \Delta_c &= \Delta_c^\circ - \frac{m}{\mu} k(t) e_{\omega_z}, \\ M_z &= M_z^\circ + (J_z e_{v_y} + m l_f e_{\omega_z}) k(t), \end{aligned} \tag{10}$$

with Δ_c°, M_z° as in (8). Although the system in (9) is time-varying, the origin is GES, as can be verified by considering the Lyapunov function $V = e_{v_y}^2 + e_{\omega_z}^2$. In the remainder of this section, the optimal value for $k(t)$ is determined.

Let $F_{yf,\mathrm{sat}}$, $M_{z,\mathrm{sat}} > 0$ be the saturation values for the AFS and RTV actuators, and define

$$\begin{aligned} u_{fp} &= \frac{F_{yf}(\alpha_{f0}) + \Delta_c}{F_{yf,\mathrm{sat}}} = \frac{F_{yf}(\alpha_{f0}) + \Delta_c^\circ}{F_{yf,\mathrm{sat}}} \\ &\qquad - \frac{m}{\mu} \frac{e_{\omega_z}}{F_{yf,\mathrm{sat}}} k(t), \\ u_{zp} &= \frac{M_z}{M_{z,\mathrm{sat}}} = \frac{M_z^\circ}{M_{z,\mathrm{sat}}} + \frac{J_z e_{v_y} + m l_f e_{\omega_z}}{M_{z,\mathrm{sat}}} k(t), \end{aligned} \tag{11}$$

where $u_{fp}, u_{zp} \in [-1, 1]$ are control quantities that are *scaled* with respect to the saturation values. The term $k(t)$ can be tuned to keep both the actuators as far away as possible from the saturation point, finding the optimal value $k^*(t)$ as the result of the following optimization problem

$$k^*(t) = \arg \min_{k(t) \in \mathbb{R}} \max \Big\{ |u_{fp}|, |u_{zp}| \Big\} = \arg \min_{k(t) \in \mathbb{R}} \|u_p\|_\infty \tag{12}$$

to be solved on–line, with $\| \cdot \|_\infty$ the infinity norm and $u_p = (u_{fp}, u_{zp})^T$. We note that, for $e_{v_y} = e_{\omega_z} = 0$ (perfect tracking), the two normalized actuations in (11) are independent of $k(t)$, so that the problem (12) has no solution, in general. The following result shows that, when $(e_{v_y}, e_{\omega_z}) \neq (0, 0)$, the solution of the problem in (12) is given by the strategy which *balances* the load on the AFS, RTV actuators.

Theorem 1: At any time t, the optimal solution $k^*(t)$ of the $\min \max$ problem (12) achieves *load balancing*, namely

$$|u_{fp}| = |u_{zp}|$$

provided that $(e_{v_y}, e_{\omega_z}) \neq (0, 0)$. ◇

Proof: The two functions in (11) are linear in $k(t)$. Hence, for the sake of a more compact notation, we define the function $\mathcal{J} : \mathbb{R} \to \mathbb{R}$ as

$$\mathcal{J}(k) = \max \Big\{ |a_1 + b_1 k|, |a_2 + b_2 k| \Big\} \tag{13}$$

and consider the equivalent optimization problem

$$\min_{k \in \mathbb{R}} \mathcal{J}(k) = \min_{k \in \mathbb{R}} \max \Big\{ |a_1 + b_1 k|, |a_2 + b_2 k| \Big\}. \tag{14}$$

We now show that there exists a global minimum point k^* of the problem in (14) also enjoying the property $|a_1 + b_1 k^*| = |a_2 + b_2 k^*|$.

Case 1: $b_1 \neq 0$, $b_2 \neq 0$. An illustration is given in Fig. 1. The two functions $|a_1 + b_1 k|$, $|a_2 + b_2 k|$ are continuous functions, piecewise–linear, unbounded above, with global minima in $-a_1/b_1$ and $-a_2/b_2$, respectively. Without loss of generality, we assume $-a_1/b_1 \leq -a_2/b_2$. Note that the function $\mathcal{J}$ in (13) is continuous on its domain and is strictly

a) decreasing for $k \in (-\infty, -a_1/b_1)$;
b) increasing for $k \in (-a_2/b_2, \infty)$.

This implies that the global minimum k^* in (14) is necessarily achieved in the compact interval $[-a_1/b_1, -a_2/b_2]$. The existence of such a minimum is ensured by the extreme value theorem. We now define the *balancing function* $B(k) = |a_2 + b_2 k| - |a_1 + b_1 k|$ and prove that $B(k^*) = 0$. We consider two sub-cases:

a) $-a_1/b_1 = -a_2/b_2$. In this case the minimum $\mathcal{J}(k^*)$ is achieved in $k^* = -a_1/b_1 = -a_2/b_2$, where both the nonnegative functions are zero and minimized. Hence $\mathcal{J}(k^*) = 0$ and $B(k^*) = 0$. The balance condition is achieved.
b) $-a_1/b_1 < -a_2/b_2$. Function B assumes the following values at the endpoints of the previously defined compact interval: $B(-a_1/b_1) = |a_2 - a_1 b_2/b_1| > 0$ and $B(-a_2/b_2) = -|a_1 - a_2 b_1/b_2| < 0$. Bolzano's theorem ensures there is a point $\bar{k}$ in the open interval $(-a_1/b_1, -a_2/b_2)$ satisfying $B(\bar{k}) = 0$, i.e. achieving balancing. Note that $\bar{k}$ is the unique point in the open interval satisfying $B(\bar{k}) = 0$, since $B(k)$ is a strictly decreasing linear function, with derivative $-|b_1| - |b_2|$, in the open interval $(-a_1/b_1, -a_2/b_2)$. We claim that $\bar{k}$ is the unique global minimum of $\mathcal{J}(k)$, namely $k^* = \bar{k}$. Note that, by Fermat's theorem, there are no local minima of $\mathcal{J}(k)$:

   i. in $(-a_1/b_1, \bar{k})$, since in this open interval the function $\mathcal{J}(k) = |a_2 + b_2 k|$ is a strictly decreasing linear function, with derivative equal to $-|b_2| < 0$;
   ii. in $(\bar{k}, -a_2/b_2)$, since in this open interval the function $\mathcal{J}(k) = |a_1 + b_1 k|$ is a strictly increasing linear function, with derivative equal to $|b_1| > 0$.

   Therefore, the optimum of $\mathcal{J}(k)$ is necessarily achieved either at $\bar{k}$, since it is the unique point where $\mathcal{J}$ is not differentiable, or at the endpoints, i.e. $k^* \in \{-a_1/b_1, \bar{k}, -a_2/b_2\}$. Finally note that, since $\mathcal{J}$ is piecewise–linear, the value of $\mathcal{J}$ at $\bar{k}$ can be expressed in terms of the values assumed at the endpoints of the

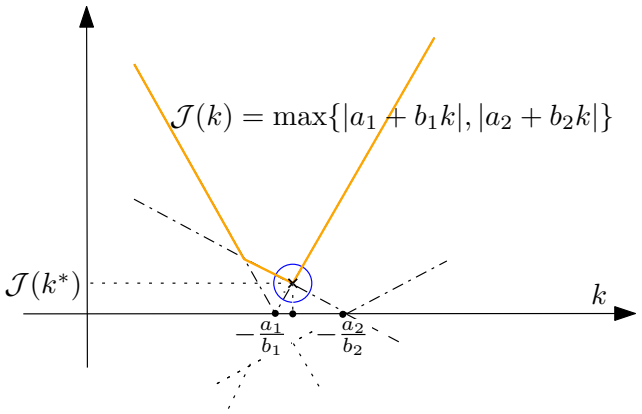

Fig. 1. Illustration of the proof of Theorem 1 (Case 1: $b_1, b_2 \neq 0$). The plot is given for $|b_1| \neq |b_2|$ and $-a_1/b_1 < -a_2/b_2$. The optimum point k^* is unique and is a point of intersection of functions $|a_1 + b_1 k|$ and $|a_2 + b_2 k|$, hence it achieves balancing: $|a_1 + b_1 k^*| = |a_2 + b_2 k^*|$.

open interval

$$\mathcal{J}(\bar{k}) = \underbrace{\mathcal{J}(-a_1/b_1) - |b_2|\overbrace{\left(\bar{k} + \frac{a_1}{b_1}\right)}^{>0}}_{<\mathcal{J}(-a_1/b_1)}$$
$$= \underbrace{\mathcal{J}(-a_2/b_2) - |b_1|\overbrace{\left(-\frac{a_2}{b_2} - \bar{k}\right)}^{>0}}_{<\mathcal{J}(-a_2/b_2)}.$$

Hence, $\bar{k}$ is the unique global minimum point of $\mathcal{J}(k)$, which concludes the proof of Case 1.

Case 2: $b_1 = 0$ or $b_2 = 0$. An illustration is given in Fig. 2. We have two sub-cases:

a) $b_1 = 0$. The min max problem is restated as

$$\min_{k\in\mathbb{R}} \mathcal{J}(k) = \min_{k\in\mathbb{R}} \max\Big\{|a_1|, |a_2 + b_2 k|\Big\} = |a_1|$$

and the optimum is achieved for any $k \in [-a_2/b_2 - |a_1/b_2|, -a_2/b_2 + |a_1/b_2|]$, so it is not unique. Anyway, the endpoints of the interval of the optimum points still achieve load balancing

$$B\left(-\frac{a_2}{b_2} \pm \left|\frac{a_1}{b_2}\right|\right) = \left|a_2 + b_2\left(-\frac{a_2}{b_2} \pm \left|\frac{a_1}{b_2}\right|\right)\right| - |a_1| = 0.$$

b) $b_2 = 0$. The min max problem is restated as

$$\min_{k\in\mathbb{R}} \mathcal{J}(k) = \min_{k\in\mathbb{R}} \max\Big\{|a_1 + b_1 k|, |a_2|\Big\} = |a_2|$$

and the optimum is achieved for any $k \in [-a_1/b_1 - |a_2/b_1|, -a_1/b_1 + |a_2/b_1|]$, so it is not unique. Anyway, the endpoints of the interval of the optimum points still achieve load balancing

$$B\left(-\frac{a_1}{b_1} \pm \left|\frac{a_2}{b_1}\right|\right) = |a_2| - \left|a_1 + b_1\left(-\frac{a_1}{b_1} \pm \left|\frac{a_2}{b_1}\right|\right)\right| = 0.$$

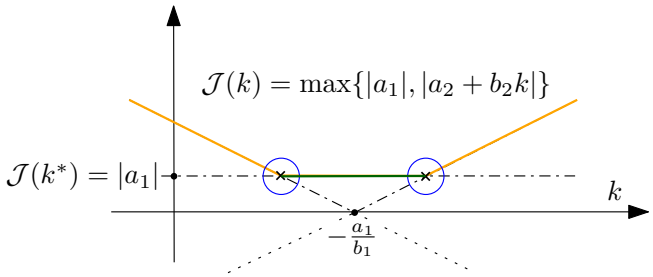

Fig. 2. Illustration of the proof of Theorem 1 (Case 2: $b_1 = 0$ or $b_2 = 0$). The plot is given for the case $b_1 = 0$ (the case $b_2 = 0$ is symmetric). The set of optimum points is a closed interval. Hence the endpoints of the interval are optimum points and are the intersections of functions $|a_1|$ and $|a_2 + b_2 k|$, hence they achieve balancing: $|a_1| = |a_2 + b_2 k^*|$.

As already noted, the case $b_1 = b_2 = 0$ corresponds to the case $e_{v_y} = e_{\omega_z} = 0$, which will not be considered since no solution exists, in general. This concludes the proof. ■

The following result characterizes the optimal gain and the optimal percentage of actuation of the balanced control strategy. The proof is omitted.

Proposition 1: For the ease of notation, define the time–varying quantities

$$a_1 = \frac{F_{yf}(\alpha_{f0}) + \Delta_c^\circ}{F_{yf,\text{sat}}}, \quad b_1 = -\frac{m}{\mu}\frac{e_{\omega_z}}{F_{yf,\text{sat}}},$$
$$a_2 = \frac{M_z^\circ}{M_{z,\text{sat}}}, \qquad b_2 = \frac{J_z e_{v_y} + m l_f e_{\omega_z}}{M_{z,\text{sat}}},$$

and the interval

$$\mathcal{I} = \begin{cases} [\alpha, \beta] & \text{if } b_1, b_2 \neq 0 \\ \mathbb{R} & \text{otherwise} \end{cases}$$

with $\alpha = \min\big\{-a_1/b_1, -a_2/b_2\big\}$, $\beta = \max\big\{-a_1/b_1, -a_2/b_2\big\}$, and assume $(b_1, b_2) \neq (0, 0)$. Then

1. The optimal gain $k^*(t)$ in (12) belongs to the set $\mathcal{I}^*$ defined as

$$\mathcal{I}^* = \begin{cases} \left\{\frac{a_2 - a_1}{b_1 - b_2}\right\} & \text{if } b_1 = -b_2 \\ \left\{\frac{-a_2 - a_1}{b_1 + b_2}\right\} & \text{if } b_1 = b_2 \\ \mathcal{I} \cap \left\{\frac{a_2 - a_1}{b_1 - b_2}, \frac{-a_2 - a_1}{b_1 + b_2}\right\} & \text{otherwise.} \end{cases} \quad (15)$$

2. The optimum balanced percentage of actuation in (12) is given by

$$\|u_p^*\|_\infty = |u_{fp}^*| = |u_{zp}^*| = \frac{|a_1 b_2 - a_2 b_1|}{|b_1| + |b_2|}. \qquad \diamond \quad (16)$$

Remark 1: The following comments are in order:

- The quantities a_1, a_2, b_1, b_2 are continuous with respect to v_y, ω_z, e_{v_y}, e_{ω_z}, Δ_c°, M_z°, δ_d. Since all these quantities are continuous in time, then a_1, a_2, b_1, b_2 are continuous in time.

Preprint submitted to 52nd IEEE Conference on Decision and Control .
Received March 11, 2013.

- The optimal gain $k^*(t)$ in (15) is uniquely defined unless $b_1 = 0$ or $b_2 = 0$. When this happens, the set $\mathcal{I}^*$ contains two optimal values (see Fig. 2), among which $k^*(t)$ can be arbitrarily chosen, and jump discontinuities in the optimal gain function may occur, in general. Anyway the optimal balanced percentage $\|u_p^*\|_\infty$ in (16) is continuous at any time.
- The balanced actuations Δ_c and M_z are computed by plugging the optimal gain $k^*(t)$ in (15) into (10); to prevent jump discontinuities in Δ_c and M_z, as a consequence of the discontinuity of the optimal gain, the computed inputs can be low-pass filtered in a real implementation.
- The optimal gain $k^*(t)$ is bounded, as shown in the proof of Theorem 1. Hence, the balanced actuations are bounded at any time. ◇

Even in the case of load balancing, one can get $\|u_p\| = 1$ at some time t in the evolution of the system. When that happens, we enter the saturation condition with both the actuators. The next section addresses the systematic design of the reference generator in order to avoid this situation.

IV. Tracking in the presence of actuator saturation: the reference generator as an additional control input

In the presence of actuator saturation, the reference generator can be adapted to impose less stringent references, with the aim of avoiding such an issue. In fact, the role of the reference generator is to generate trajectories that can be actually followed by the real vehicle. Therefore, there is no reason to generate impractical references, determining actuator saturation, since in this case the real vehicle cannot track those trajectories.

In the following, we propose two different ways of modifying the reference generator and we also quantify the reference modifications in terms of the amount of computed control action which cannot be exerted. The method is independent of the reference dynamics which is used in the case of non-saturating actuators.

Case 1: Additive terms. In this first case, one adds some fictitious forces Δ_f, Δ_r, which can be regarded as additional inputs, to be imposed in order to avoid actuator saturation. The proposed reference generator is the following

$$\begin{aligned}\dot{v}_{y,\mathrm{ref}} &= -v_x\omega_{z,\mathrm{ref}} + \frac{\mu}{m}\Big(F_{yf,\mathrm{ref}}(\alpha_{f0,\mathrm{ref}}) + \Delta_f \\ &\qquad + F_{yr,\mathrm{ref}}(\alpha_{r,\mathrm{ref}}) + \Delta_r\Big), \\ \dot{\omega}_{z,\mathrm{ref}} &= \frac{\mu}{J_z}\Big(F_{yf,\mathrm{ref}}(\alpha_{f0,\mathrm{ref}})l_f + \Delta_f l_f \\ &\qquad - F_{yr,\mathrm{ref}}(\alpha_{r,\mathrm{ref}})l_r - \Delta_r l_r\Big),\end{aligned} \tag{17}$$

with $\alpha_{f0,\mathrm{ref}}$, $\alpha_{r,\mathrm{ref}}$ as in (5). From (3), (4), (17), the tracking error dynamics become

$$\begin{aligned}\dot{e}_{v_y} &= -v_x e_{\omega_z} + \frac{\mu}{m}(E_f - \Delta_f + E_r - \Delta_r) + \frac{\mu}{m}\Delta_c, \\ \dot{e}_{\omega_z} &= \frac{\mu}{J_z}(E_f l_f - \Delta_f l_f - E_r l_r + \Delta_r l_r) \\ &\qquad + \frac{\mu l_f}{J_z}\Delta_c + \frac{1}{J_z}M_z,\end{aligned}$$

with E_f, E_r as in (7). By imposing the dynamics (9), one gets

$$\begin{aligned}\Delta_c &= \Delta_c^\circ - \frac{m}{\mu}k^*(t)e_{\omega_z} + \Delta_f + \Delta_r, \\ M_z &= M_z^\circ + (J_z e_{v_y} + m l_f e_{\omega_z})k^*(t) - \mu(l_f + l_r)\Delta_r,\end{aligned}$$

with Δ_c°, M_z° as in (8) and $k^*(t)$ being the solution of the optimal problem (12). From the definition (2), and considering the *scaled* control quantities

$$\begin{aligned}u_{fp}^\Delta &= u_{fp}^* + \frac{\Delta_f + \Delta_r}{F_{yf,\mathrm{sat}}}, \\ u_{zp}^\Delta &= u_{zp}^* - \mu\frac{(l_f + l_r)\Delta_r}{M_{z,\mathrm{sat}}},\end{aligned}$$

with u_{fp}^*, u_{zp}^* being the optimum values of u_{fp}, u_{zp} in (11) for $k(t) = k^*(t)$, one can determine Δ_f, Δ_r by imposing $u_{fp}^\Delta, u_{zp}^\Delta \in [-1, 1]$, so obtaining

$$\Delta_r = \begin{cases} (u_{zp}^* - 1)\dfrac{M_{z,\mathrm{sat}}}{\mu(l_f + l_r)} & \text{if } u_{zp}^* > 1, \\ 0 & \text{if } u_{zp}^* \in [-1, 1], \\ (u_{zp}^* + 1)\dfrac{M_{z,\mathrm{sat}}}{\mu(l_f + l_r)} & \text{if } u_{zp}^* < -1, \end{cases}$$

$$\Delta_f = \begin{cases} (1 - u_{fp}^*)F_{yf,\mathrm{sat}} - \Delta_r & \text{if } u_{fp}^* > 1, \\ -\Delta_r & \text{if } u_{fp}^* \in [-1, 1], \\ -(1 + u_{fp}^*)F_{yf,\mathrm{sat}} - \Delta_r & \text{if } u_{fp}^* < -1. \end{cases}$$

Case 2: Multiplicative terms. In this second case, one considers some fictitious friction coefficients $\lambda_f, \lambda_r \in [0, 1]$, which can be regarded as additional inputs, "fading" the tyre forces in order to avoid actuator saturation. Therefore, the proposed reference generator is the following

$$\begin{aligned}\dot{v}_{y,\mathrm{ref}} &= -v_x\omega_{z,\mathrm{ref}} + \frac{\mu}{m}\Big(\lambda_f F_{yf,\mathrm{ref}}(\alpha_{f0,\mathrm{ref}}) \\ &\qquad + \lambda_r F_{yr,\mathrm{ref}}(\alpha_{r,\mathrm{ref}})\Big), \\ \dot{\omega}_{z,\mathrm{ref}} &= \frac{\mu}{J_z}\Big(\lambda_f F_{yf,\mathrm{ref}}(\alpha_{f0,\mathrm{ref}})l_f - \lambda_r F_{yr,\mathrm{ref}}(\alpha_{r,\mathrm{ref}})l_r\Big),\end{aligned} \tag{18}$$

with $\alpha_{f0,\mathrm{ref}}$, $\alpha_{r,\mathrm{ref}}$ as in (5). From (3), (4), (18), the tracking error dynamics become

$$\begin{aligned}\dot{e}_{v_y} &= -v_x e_{\omega_z} + \frac{\mu}{m}(F_{yf} - \lambda_f F_{yf,\mathrm{ref}} + F_{yr} - \lambda_r F_{yr,\mathrm{ref}}) \\ &\qquad + \frac{\mu}{m}\Delta_c, \\ \dot{e}_{\omega_z} &= \frac{\mu}{J_z}(F_{yf}l_f - \lambda_f F_{yf,\mathrm{ref}}l_f - F_{yr}l_r + \lambda_r F_{yr,\mathrm{ref}}l_r) \\ &\qquad + \frac{\mu l_f}{J_z}\Delta_c + \frac{1}{J_z}M_z,\end{aligned}$$

Preprint submitted to 52nd IEEE Conference on Decision and Control .
Received March 11, 2013.

with E_f, E_r as in (7). By imposing the dynamics (9), one gets

$$\begin{aligned}\Delta_c &= \Delta_c^\circ - \frac{m}{\mu}k^*(t)e_{\omega_z} - (1-\lambda_f)F_{yf,\mathrm{ref}} \\ &\quad - (1-\lambda_r)F_{yr,\mathrm{ref}}, \\ M_z &= M_z^\circ + (J_z e_{v_y} + m l_f e_{\omega_z})k^*(t) \\ &\quad + \mu(l_f+l_r)(1-\lambda_r)F_{yr,\mathrm{ref}},\end{aligned}$$

with Δ_c°, M_z° as in (8) and $k^*(t)$ being the solution of the optimal problem (12). As in the previous case, from the definition (2), and considering the *scaled* control quantities

$$\begin{aligned}u_{fp}^\lambda &= u_{fp}^* - \frac{(1-\lambda_f)F_{yf,\mathrm{ref}} + (1-\lambda_r)F_{yr,\mathrm{ref}}}{F_{yf,\mathrm{sat}}}, \\ u_{zp}^\lambda &= u_{zp}^* + \mu\frac{(l_f+l_r)(1-\lambda_r)F_{yr,\mathrm{ref}}}{M_{z,\mathrm{sat}}},\end{aligned}$$

with u_{fp}^*, u_{zp}^* being the optimum values of u_{fp}, u_{zp} in (11) for $k(t) = k^*(t)$, one can determine λ_f, λ_r by imposing $u_{fp}^\lambda, u_{zp}^\lambda \in [-1,1]$, so obtaining

$$\lambda_r = \begin{cases} 1 + (u_{zp}^* - 1)\dfrac{M_{z,\mathrm{sat}}}{\mu(l_f+l_r)F_{yr,\mathrm{ref}}} & \text{if } u_{zp}^* > 1, \\ 1 & \text{if } u_{zp}^* \in [-1,1], \\ 1 + (u_{zp}^* + 1)\dfrac{M_{z,\mathrm{sat}}}{\mu(l_f+l_r)F_{yr,\mathrm{ref}}} & \text{if } u_{zp}^* < -1, \end{cases}$$

$$\lambda_f = \begin{cases} 1-(u_{fp}^*-1)\dfrac{F_{yf,\mathrm{sat}}}{F_{yf,\mathrm{ref}}} + (1-\lambda_r)\dfrac{F_{yr,\mathrm{ref}}}{F_{yf,\mathrm{ref}}} & \text{if } u_{fp}^* > 1, \\ 1+(1-\lambda_r)\dfrac{F_{yr,\mathrm{ref}}}{F_{yf,\mathrm{ref}}} & \text{if } u_{fp}^* \in [-1,1], \\ 1-(u_{fp}^*+1)\dfrac{F_{yf,\mathrm{sat}}}{F_{yf,\mathrm{ref}}} + (1-\lambda_r)\dfrac{F_{yr,\mathrm{ref}}}{F_{yf,\mathrm{ref}}} & \text{if } u_{fp}^* < -1. \end{cases}$$

V. Simulation results

In this section, we provide simulation results of the proposed control techniques. We consider two simulation sets. First, we show some results about the balanced nonlinear controller described in Section III. Then, we show the performance of the controller with adaptive reference generation in the presence of actuator saturation, illustrated in Section IV.

The parameters of the vehicle are equal to

$$\begin{array}{lll} m = 1550 \text{ kg} & l_f = 1.17 \text{ m} & l_r = 1.43 \text{ m} \\ M_{z,\mathrm{sat}} = 10000 \text{ Nm} & J_z = 2300 \text{ kg}\cdot\text{m}^2 & \mu = 1 \\ F_{yf,\mathrm{sat}} = 8854 \text{ N} & F_{yr,\mathrm{sat}} = 8394 \text{ N} & \end{array}$$

and we set $k_1 = k_2 = 1$ in the error dynamics (9). The tire lateral force functions are given by [12]

$$\begin{aligned}F_{y,f}(\alpha_f) &= C_{y,f}\sin(A_{y,f}\arctan(B_{y,f}\alpha_f)) \\ F_{y,r}(\alpha_r) &= C_{y,r}\sin(A_{y,r}\arctan(B_{y,r}\alpha_r))\end{aligned} \tag{19}$$

where $A_{y,f} = 1.81$, $A_{y,r} = 1.68$, $B_{y,f} = 7.2$, $B_{y,r} = 11$, $C_{y,f} = F_{yf,\mathrm{sat}}$, $C_{y,r} = F_{yr,\mathrm{sat}}$.

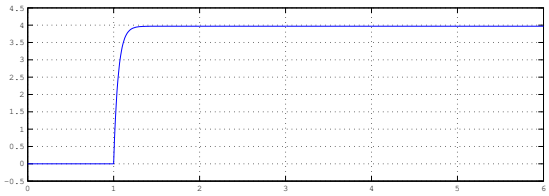

Fig. 3. Driver wheel angle [rad] vs time [s].

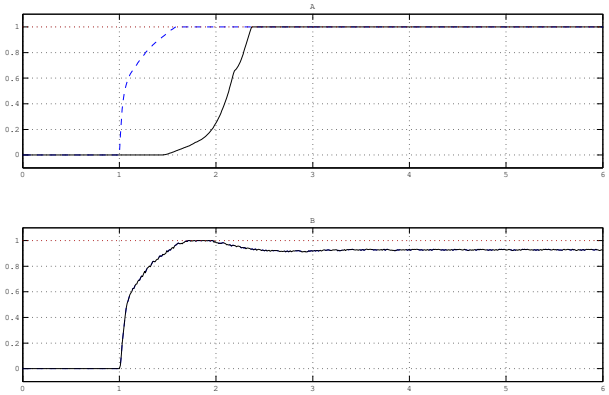

Fig. 4. Percentage of actuation vs time [s]. Case A) - Vehicle with nominal controller: $|u_{fp}|$ (blue dashed line) and $|u_{zp}|$ (black solid line). Case B) - Vehicle with balanced controller: $|u_{fp}|$ (blue dashed line) and $|u_{zp}|$ (black solid line).

The nominal reference generator is assumed to have the same vehicle parameters but different tire functions, ensuring global asymptotic stability of the reference dynamics. Further details about the reference generation are given in [10].

A. Performance of the balanced nonlinear controller

The first test maneuver is a step steer of $65°$ with longitudinal velocity of 35 m/s (see Fig. 3). In Figures 4, 5 and 6 we show, respectively, the percentage of actuation, the state variables and the planar trajectory in the case of vehicle controlled by means of the nominal controller (Section III-A) and in the case of vehicle controlled by balancing the actuators (Section III-B). The step steer occurs at time $t = 1$. The nominal controller (Fig. 4-A) reacts by means of the AFS actuation, which rapidly enters the saturation condition. After that, the RTV is increased to compensate the lack of tracking. At time $t = 2.2$, the RTV is saturated and the tracking is lost. The balanced controller (Fig. 4-B), instead, provides the same percentage of actuation with both the inputs. At time $t = 1.8$, the saturation is reached but the whole control action is recovered after $t = 2$ and the tracking is achieved (see Figures 5–6). Note from Fig. 4-B that the steady-state percentage of actuation $\|u_p^*\|_\infty$ is about 0.95 (i.e. the 95% of the available control), which indicates a rather hard cornering maneuver, yet feasible by balancing the control effort.

Preprint submitted to 52nd IEEE Conference on Decision and Control .
Received March 11, 2013.

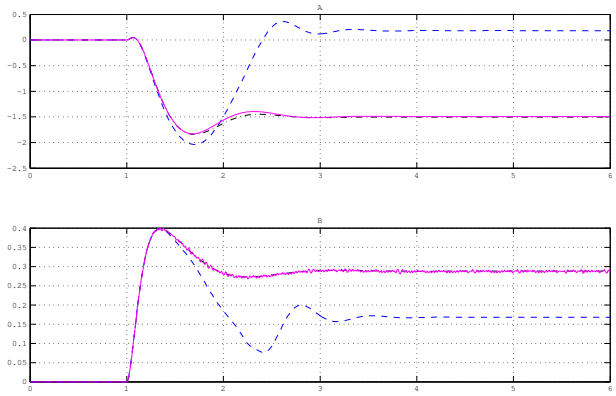

Fig. 5. Panel A) - v_y [m/s] vs time [s]: reference (black dash-dotted line), nominal controller (blue dashed line) and balanced controller (magenta solid line); Panel B) - ω_z [rad/s] vs time [s]: reference (black dash-dotted line), nominal controller (blue dashed line) and balanced controller (magenta solid line).

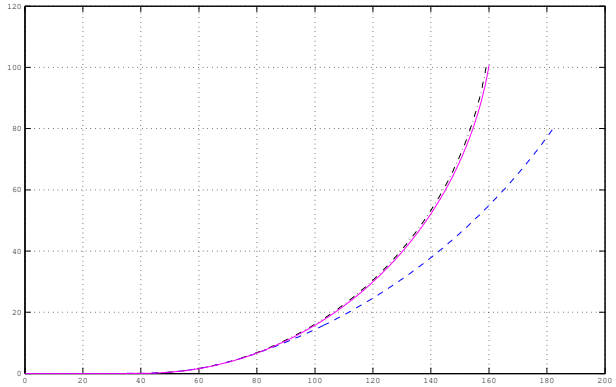

Fig. 6. Trajectory in the plane: reference (black dash-dotted line), nominal controller (blue dashed line) and balanced controller (magenta solid line).

B. *Performance of the reference adaptation*

We now consider the balanced controller in Section III and we compare the behavior of a vehicle following a reference generator designed for nominal conditions to the behavior of a vehicle whose reference is adapted by means of the adaptive technique presented in Section IV. For lack of space, we just consider Case 1 of Section IV, using additive terms in the reference.

The test maneuver considered is a double step steer (see input driver in Fig. 7) of 100° with longitudinal velocity of 35 m/s. Such a maneuver is very hard and the control actuators are in saturation most of the time (see Fig. 8).

Figures 9–10 show that the ideal reference trajectory is too strict and causes the instability of the vehicle controlled by means of the balanced controller without reference adaptation. On the contrary, the adapted reference trajectory looks feasible and the corresponding vehicle has a stable behavior, also achieving a good tracking, in spite of the very hard maneuver imposed by the driver.

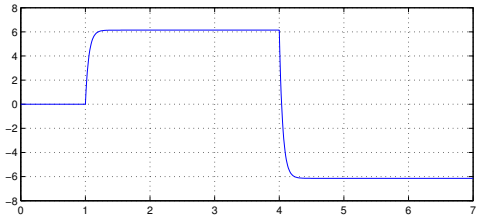

Fig. 7. Driver wheel angle [rad] vs time [s].

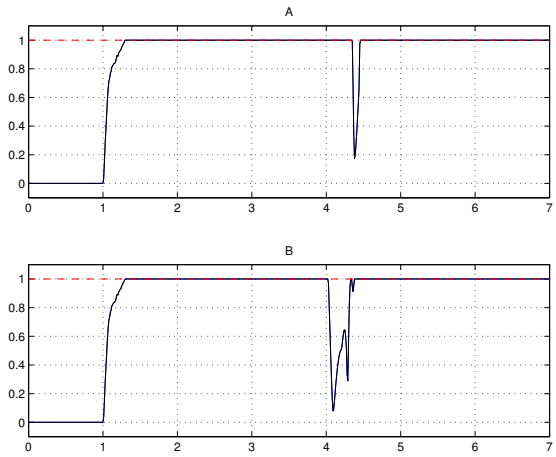

Fig. 8. Percentage of actuation vs time [s]. Case A) - Vehicle with balanced controller without reference adaptation: $|u_{fp}|$ (blue dashed line) and $|u_{zp}|$ (black solid line). Case B) - Vehicle with balanced controller and reference adaptation: $|u_{fp}|$ (blue dashed line) and $|u_{zp}|$ (black solid line).

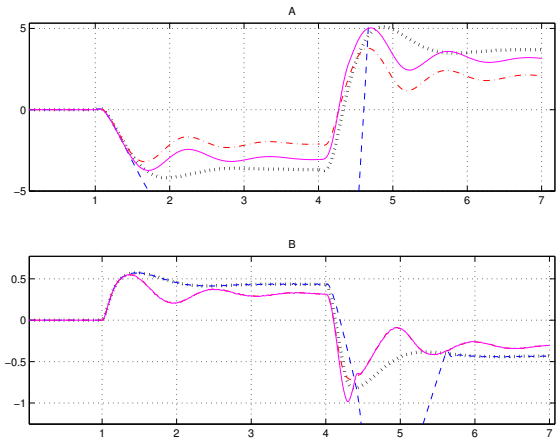

Fig. 9. Panel A) - v_y [m/s] vs time [s]: nominal reference (black dotted line), balanced controller without reference adaptation (blue dashed line), adapted reference (red dash-dotted line), balanced controller with reference adaptation (magenta solid line); Panel B) - ω_z [rad/s] vs time [s]: nominal reference (black dotted line), balanced controller without reference adaptation (blue dashed line), adapted reference (red dash-dotted line), balanced controller with reference adaptation (magenta solid line).

Preprint submitted to 52nd IEEE Conference on Decision and Control .
Received March 11, 2013.

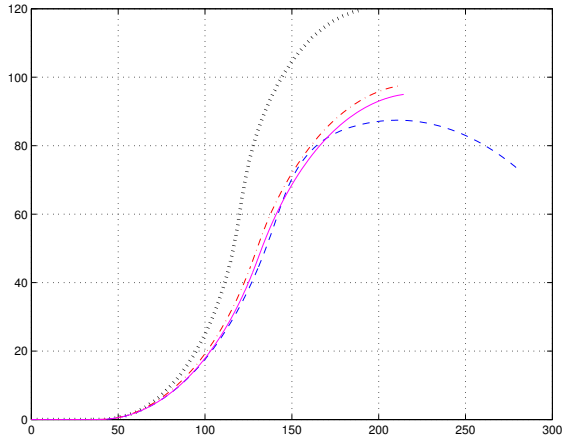

Fig. 10. Trajectory in the plane: nominal reference (black dotted line), balanced controller without reference adaptation (blue dashed line), adapted reference (red dash-dotted line), balanced controller with reference adaptation (magenta solid line).

VI. Conclusions

In this paper, we addressed the topic of vehicle attitude control by means of Active Front Steer And Rear Torque Vectoring, in the presence of actuator saturation. We proposed a balancing approach for the design of a nonlinear control law achieving the tracking goal while keeping the vehicle far from saturation. This was obtained by redistributing the workload on the actuators. Anyway, in hard maneuvers, saturations may still occur even in the presence of a balancing controller. In order to avoid this issue, the reference is adapted to prevent the lack of control action. Simulations show the effectiveness of the proposed method.

Improvements of the results, taking into account parameter uncertainties, are currently under study. Furthermore, we plan to extend the simulation setup by means of a more realistic simulation environment (such as a commercially available industrial simulator), in order to show the robustness of the proposed approach.

References

[1] G. Burgio, and P. Zegelaar, Integrated Vehicle Control Using Steering and Brakes, *International Journal of Control*, Vol. 79, No. 2, pp. 162–169, 2006.

[2] P. Setlur, J. R. Wagner, D. M. Dawson, and D. Braganza, A Trajectory Tracking Steer–by–Wire Control System for Ground Vehicles, *IEEE Transactions on Vehicular Technology*, Vol. 55, No. 1, pp. 76–85, 2006.

[3] J. Ackermann, J. Guldner, R. Steinhausner, and V. Utkin, Linear and nonlinear design for robust automatic steering, *IEEE Transactions on Control System Technology*, Vol. 3, No. 1, pp. 132–143, 1995.

[4] S. Malan, M. Taragna, P. Borodani, and L. Gortan, Robust performance design for a car steering device, *Proceedings of the* 33^{rd} *IEEE Conference on Decision and Control*, Lake Buena Vista, FL, USA, pp. 474–479, 1994.

[5] D. Bianchi, A. Borri, G. Burgio, M. D. Di Benedetto, and S. Di Gennaro, Adaptive Integrated Vehicle Control using Active Front Steering and Rear Torque Vectoring, *Proceedings of the joint* 48^{th} *IEEE Conference on Decision and Control and* 28^{th} *Chinese Control Conference (CDC-CCC 2009)*, Shanghai, China, pp. 3557-3562, 2009.

[6] D. Bianchi, A. Borri, G. Burgio, M. D. Di Benedetto, and S. Di Gennaro, Adaptive Integrated Vehicle Control using Active Front Steering and Rear Torque Vectoring, *International Journal of Vehicle Autonomous Systems*, Special Issue on: "Autonomous and Semi–Autonomous Control for Safe Driving of Ground Vehicles", Vol. 8, No. 2/3/4, pp. 85–105, 2010.

[7] L. Zaccarian, and M. Turner, Special issue on antiwindup, *International Journal of Systems Science*, 37(2), 2006.

[8] A. Glattfelder, Y. Ohta, E. Mosca, and S. W. Weiland, Special issue on anti–windup control, *European Journal of Control*, 6(5), 403-380, 2000.

[9] M. Canale, L. Fagiano, M. Milanese, P. Borodani, Robust vehicle yaw control using an active differential and IMC techniques, *Control Engineering Practice*, Vol. 15, No. 8, pp. 923–94, 2007

[10] D. Bianchi, A. Borri, B. Castillo–Toledo, M. D. Di Benedetto, and S. Di Gennaro, Active Control of Vehicle Attitude with Roll Dynamics, *Proceedings of the* 18^{th} *IFAC World Congress*, Milan, Italy, pp. 7174-7179, 2011.

[11] D. Bianchi, A. Borri, B. Castillo–Toledo, M. D. Di Benedetto, and S. Di Gennaro, Smart Management of Actuator Saturation in Integrated Vehicle Control, *Proceedings of the* 50^{th} *IEEE Conference on Decision and Control and European Control Conference (CDC-ECC 2011)*, Orlando, FL, USA, pp. 2529-2534, 2011.

[12] H. Pacejka, *Tyre and Vehicle Dynamics*, Elsevier Butterworth–Heinemann, 2005.

[13] R. Rajamani, *Vehicle Dynamics and Control*, Mechanical Engineering Series, Springer–Verlag, 2006.

Preprint submitted to 52nd IEEE Conference on Decision and Control .
Received March 11, 2013.